

Solution Casting and Transfer Printing Single-Walled Carbon Nanotube Films

Matthew A. Meitl,^{†,‡,§,||} Yangxin Zhou,^{†,‡,§,||} Anshu Gaur,^{†,‡,§,||} Seokwoo Jeon,^{†,‡,§,||}
Monica L. Usrey,^{⊥,§,||} Michael S. Strano,^{⊥,§,||} and John A. Rogers^{*,†,‡,§,||}

Department of Materials Science and Engineering, Department of Chemistry, Beckman Institute, Seitz Materials Research Laboratory, and Department of Chemical and Biomolecular Engineering, University of Illinois at Urbana/Champaign, Urbana, Illinois 61801

Received May 28, 2004

ABSTRACT

This paper presents methods for solution casting and transfer printing collections of individual single-walled carbon nanotubes (SWNTs) onto a wide range of substrates, including plastic sheets. The deposition involves introduction of a solvent that removes surfactant from a suspension of SWNTs as it is applied to a substrate. The subsequent controlled flocculation (cF) produces films of SWNTs with densities that can be varied between a few tubes per square micron to thick multilayers in a single deposition step and with orientation determined by the direction of solution flow. High-resolution rubber stamps inked in this manner can be used to print patterns of tubes with geometries defined by the relief structure on the surface of the stamp. Thin film transistors fabricated with these techniques demonstrate their potential use in flexible “macroelectronic” systems.

The remarkable properties of single-walled carbon nanotubes (SWNTs) motivate research efforts to understand their fundamental nature and to explore their potential for commercial applications. Extraordinarily high mobilities in semiconducting SWNTs¹ and their capacity to support large current densities² make them potentially valuable as semiconductors and interconnects in nanoscale electronic circuits. Applications also exist in the emerging area of flexible plastic electronics, or “macroelectronic” systems, where large collections (arrays or random networks) of SWNTs form effective semiconductors in thin-film transistors (TFTs)^{3–6} or transparent conductors.⁷ Successful implementation of SWNTs for these applications requires methods to deposit and pattern them over large areas, at high resolution, and with processing temperatures that are compatible with plastics. To obtain good electrical properties, the resulting SWNT films must be composed of clean, exfoliated, aligned, and undamaged tubes with controlled surface coverage. Conventional high-temperature chemical vapor deposition growth followed by casting and transfer to plastic backing layers⁵ represents one method for integrating tubes with flexible substrates. Langmuir–Blodgett techniques,^{8–11} dry transfer methods,¹² and various schemes of deposition from solution^{13–22} have the advantage that they can be scaled to

large areas. They also provide some patterning and/or alignment capability, but each has certain disadvantages, including the use of organic solvents that are incompatible with many plastics.^{16,18} Previously described techniques for depositing SWNT films from aqueous solution generally yield low coverages^{11,14,15,17} or rely on slow procedures or repeated depositions²⁰ to increase SWNT film density. Many techniques rely on chemical modification of the SWNTs^{7–9,16,19,21,22} which may degrade the electrical performance of the tubes. This paper presents new deposition and patterning methods with characteristics that match many of the requirements for application in macroelectronics. The deposition technique exploits a controlled flocculation (cF) process to deposit surfactant-stabilized nanotubes from aqueous solution onto a variety of substrates, with a wide range of surface coverages. The method can be used to “ink” high-resolution rubber stamps which can then be used to form patterns of tubes by dry-transfer printing. Thin film transistors represent simple structures that can be fabricated in this manner.

Figure 1 illustrates the methods. The cF process employs a “dual spinning” approach in which a suspension of tubes and an appropriate solvent (methanol in this case) are applied, at the same time, to a spinning substrate. See Figure 1a. For experiments in this work, the tube solution consists of ~50 mg/L individual HiPco SWNTs obtained from Rice University in 1 wt % aqueous sodium dodecyl sulfate (SDS). The solution was homogenized for 1 h at 6500 rpm, sonicated for 10 min, and centrifuged for 4 h at 30 000 rpm. No chemical purification was performed on the as-received tubes.

* Corresponding author: email jrogers@uiuc.edu.

[†] Department of Materials Science and Engineering.

[‡] Department of Chemistry.

[§] Beckman Institute.

^{||} Seitz Materials Research Laboratory.

[⊥] Department of Chemical and Biomolecular Engineering.

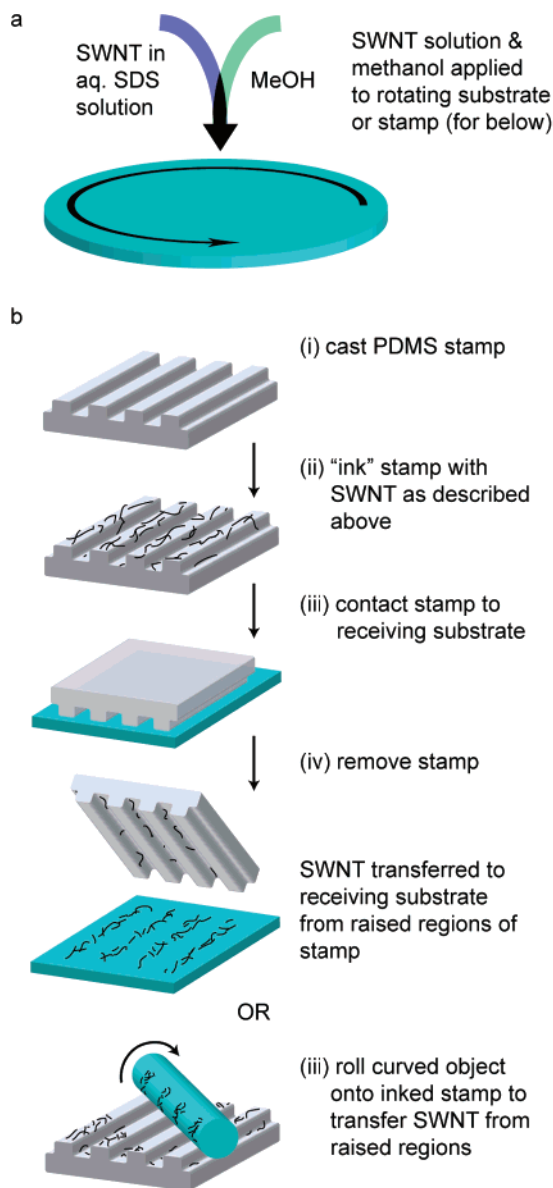


Figure 1. Experimental procedures for (a) depositing films of individual single-walled carbon nanotubes by controlled flocculation (cF) and for (b) transfer printing films deposited in this manner from the surface of a high resolution rubber stamp. (a) SWNTs stabilized in aqueous SDS solution are introduced to a rapidly rotating substrate and mixed with methanol. (b) A PDMS stamp is "inked" with SWNTs by the procedure described in (a) and then brought into contact with a substrate. SWNTs are transferred from raised regions of the stamp.

A stream of this solution and a stream of methanol are simultaneously introduced onto the center of a rotating (5000 rpm) substrate using syringes. The methanol removes the surfactant from the nanotubes and causes them to fall out of solution. Other solvents may be used in place of methanol, provided they are miscible with water and have a strong affinity for the surfactant. The spinning substrate drives the fluids to the edges, thereby controlling the time that the two fluids have to mix. If the nanotubes land on the surface before they meet each other in suspension, then a film of individual (nonbundled) SWNTs results. The deposition of SWNTs can continue indefinitely to produce thick films, not limited by

charge repulsion between the tube–surfactant complexes. This procedure, in which methanol actively drives the nanotubes out of suspension, is much different than methods that rely on attractive interactions between the tubes and specially designed surface chemistries on the substrate. As a result, the cF approach has wide applicability to substrates of different types, and it can yield high surface coverages in a single step. In fact, the cF process allows tubes to be deposited directly onto high-resolution poly(dimethylsiloxane) (PDMS) stamps formed by the techniques of soft lithography. Contacting a stamp inked in this manner to a substrate that has a higher surface energy than the PDMS leads to the efficient transfer of tubes from the raised (i.e., contacting) regions of the stamp, as illustrated in Figure 1b. As with other stamping techniques,²³ the transfer printing of SWNTs can be applied to nonplanar substrates.

Figure 2a shows atomic force microscopy (AFM) images of SWNT films deposited by cF onto SiO₂/Si substrates treated with (aminopropyl)triethoxysilane (APTS) (1 min soak in a 1 mM aq solution). Omitting the methanol yields minimal coverage (inset, Figure 2a) when otherwise similar conditions are used (i.e., substrate type, tube solution, and spinning speed). In fact, we observe coverage comparable to that of the inset in Figure 2a ($<1 \mu\text{m}^{-2}$), independent of soaking time or meniscus velocity when methanol is not used, provided the SWNT solution is not allowed to evaporate on the substrate. Desolvation of the nanotubes governs, to a large extent, the cF process. As a result, cF enables controlled SWNT deposition onto a wide range of substrates, including SiO₂ (APTS-treated and untreated), ITO, polyimide, Au, mica (APTS-treated and untreated), PDMS, and poly(methyl methacrylate) (PMMA, Figure 2b). Surface chemistry does, however, play a role in determining the uniformity and density of films. The densest and most uniform films are found on APTS-treated SiO₂. AFM line scans show that submonolayer films in all cases are composed of individual tubes and small bundles ($<1\text{--}4 \text{ nm}$, Figure 2c). Larger bundles (4–10 nm) are present in films that contain a full monolayer or more. The flow of fluid on the spinning substrate produces radial alignment of the tubes and bundles (Figure 2d). This effect is most pronounced when the direction of flow is well-defined, i.e., on larger substrates and away from the center of rotation. The optical absorbance of SWNT films deposited onto glass demonstrates this alignment even in multilayer films (Figures 2e,f). Optical anisotropy was observed in the films at $\lambda = 355 \text{ nm}$, showing an absorbance dependent upon the orientation of the film relative to the direction of polarization of the laser, ranging from 0.75% to 1.65% for a film thickness of $\sim 5 \text{ nm}$.

The capability of cF to deposit uniform SWNT films on PDMS allows transfer-printing, similar to what has been demonstrated before using DNA.^{24,25} The operational procedures for "inking" the stamp with SWNTs are identical to those for depositing onto flat substrates described above. The relief on the stamps, however, disrupts flow-induced alignment to some extent and it decreases the level of coverage uniformity. Nevertheless, it is possible to achieve printed films with good quality. An important aspect of the process

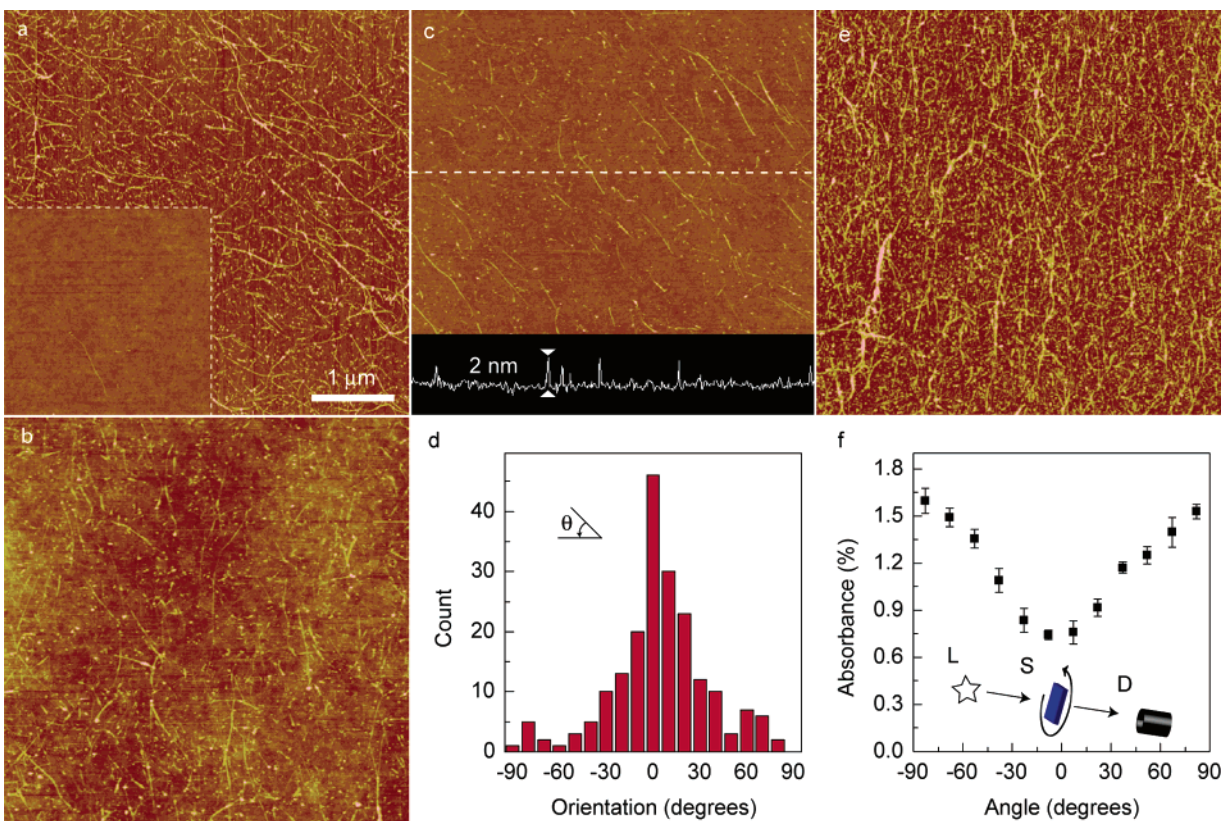


Figure 2. AFM images of SWNT films produced by cF. All scales identical. (a) Effect of methanol addition. SWNT film deposited on to APTS-treated SiO_2/Si with methanol. Inset: very low coverage in SWNT film produced by otherwise identical conditions when methanol is omitted. (b) SWNT films deposited onto plastic (PMMA on Mylar). (c) Morphology of films and inset height cross-section of scan shown by dashed line. (d) Distribution of SWNT and bundle orientations in (c). (e,f) Effect of alignment on optical absorbance. (f) Absorbance at $\lambda = 355$ nm of ~ 5 nm SWNT film on APTS-treated glass shown in (e) as the film is rotated. Inset: measurement setup of laser with well-defined polarization (L), rotating SWNT film sample (S), and detector (D).

is that it is dry; the receiving substrate is not exposed to a solvent. Figure 3 shows patterned films produced by transfer printing onto SiO_2 and PMMA. The transfer is guided by differences in surface energies of the stamps and the substrate, and it is mediated by the smoothness of the receiving surface. For example, in the case of transfer printing onto gold, transfer occurs readily onto smooth, clean gold (Au (111) on mica, SPI Inc., rms roughness = 1.1 \AA) but to a much lesser extent onto self-assembled monolayers of hexadecanethiol produced by microcontact printing on the smooth gold or onto rougher gold produced by e-beam evaporation (rms roughness = 8.36 \AA). More complete transfer of the nanotubes can be facilitated by mild heating during contact ($65 \text{ }^\circ\text{C}$ for 1–5 min). The printing can be performed multiple times on the same substrate without additional complications (Figure 3c). Figure 3d demonstrates the capability to transfer print onto the curved outer surface of a glass capillary tube (diameter $500 \mu\text{m}$) by rolling.

Thin film transistors produced with these films demonstrate their electrical properties. Standard e-beam lithography with Pd and soft-contact lamination (ScL) with Au defined contacts for these devices (Figure 4). Figure 4a shows the transfer characteristics of TFT structures fabricated on SWNT films deposited by cF with the SWNT preferentially oriented across the channel (parallel) and perpendicular to the channel. The resistivity of the film in the direction of the SWNT

alignment was found to be ~ 3 times lower ($0.08 \Omega\text{cm}$) than in the direction perpendicular to the tubes ($0.24 \Omega\text{cm}$). The current can be modulated using the underlying Si substrate as a back gate, indicating the partially semiconducting character of the film. The level of off-current can be dramatically reduced by selective electrical breakdown of the metallic pathways.^{6,26} Figure 4b displays the current–voltage (I – V) characteristics of a functional SWNT film TFT produced by ScL followed by electrical breakdown at a gate voltage of 40 V while V_{ds} is swept from 0 to 40 V. The resulting on/off ratio is improved to ~ 130 . The very low coverage of SWNT in this case was achieved by conventional deposition procedures²⁰ (i.e., it did not require the use of cF).

In conclusion, this paper introduces methods of depositing and patterning SWNT thin films. The deposition approach employs the desolvation of individual surfactant-stabilized nanotubes and allows good density control of on a wide variety of substrates with the capability of nanotube alignment. The patterning technique allows the dry transfer of SWNT films deposited on PDMS stamps to smooth substrates. Simple optical and electrical measurements on the SWNT films formed with these techniques illustrate some of their properties. Solution casting and printing techniques of the type introduced here could be useful for SWNT-based

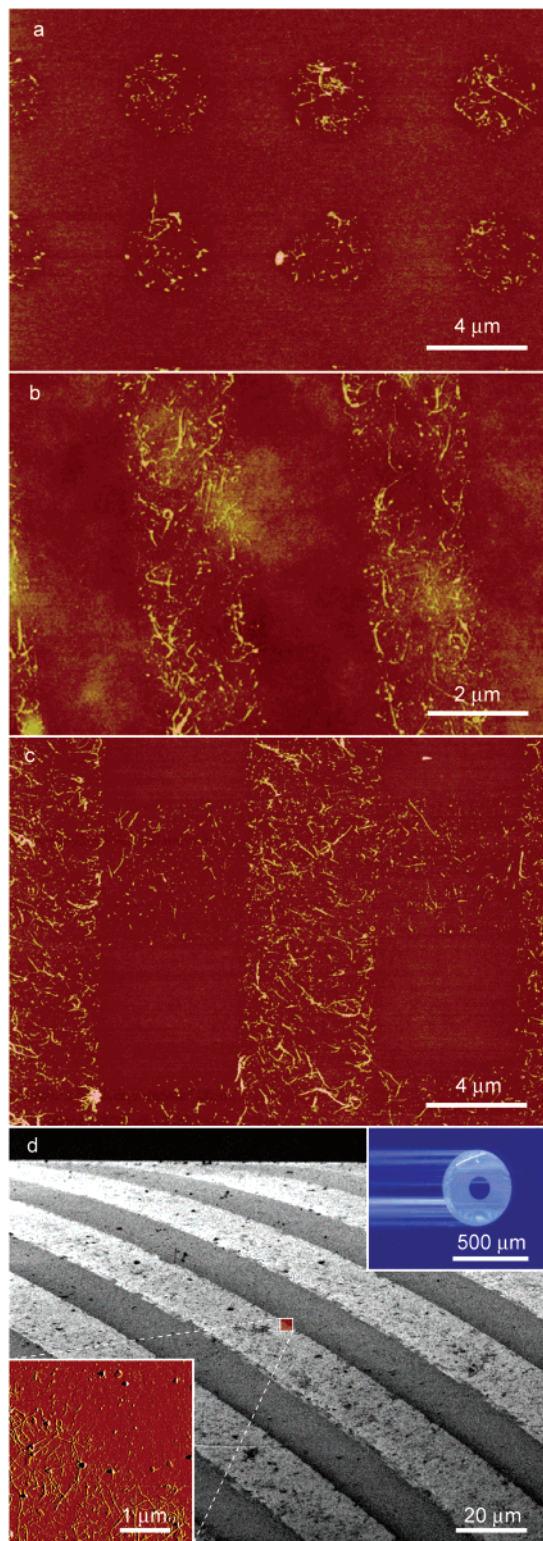


Figure 3. Transfer-printed patterns of SWNT imaged by AFM and SEM. (a) Dots printed onto APTS-treated SiO_2/Si . (b) Lines deposited onto PMMA on Mylar. (c) Cross-pattern of lines produced by two-step printing onto APTS-treated SiO_2/Si . (d) SEM image of printed lines (light) on capillary tube (dark) with outer diameter $\sim 500 \mu\text{m}$. Top-right inset: optical micrograph of capillary tube. Bottom-left inset: AFM amplitude image of SWNT film boundary on capillary tube.

macroelectronics, sensors, and other areas that require wide-area, uniform deposition of tubes.

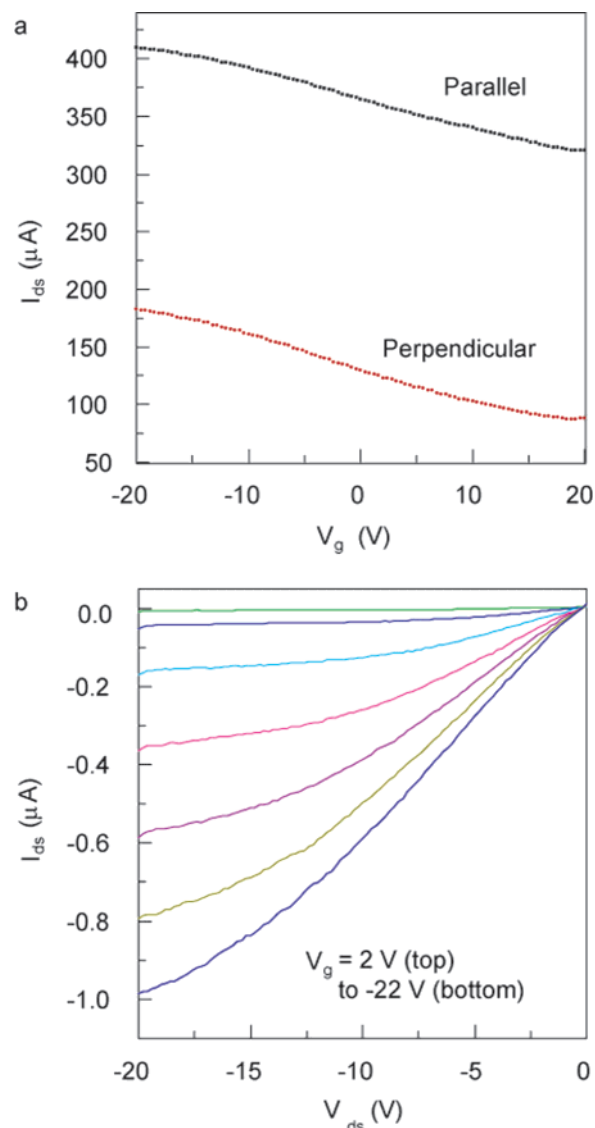


Figure 4. Electrical properties of SWNT films deposited from solution. (a) Gate modulation of source–drain current through film of SWNTs aligned across the channel (parallel) and perpendicular to channel. (b) Current–voltage (I – V) characteristics of a SWNT TFT produced by ScL followed by electrical breakdown of metallic pathways.

Acknowledgment. The authors thank Joseph W. Lyding for the use of his AFM. This work was supported by DARPA-funded AFRL-managed Macroelectronics Program Contract F8650-04-C-7101, the U.S. Department of Energy under grant DEFG02-91-ER45439, and a graduate fellowship from the Fannie and John Hertz Foundation.

References

- (1) Dürkop, T.; Getty, S. A.; Cobas, E.; Fuhrer, M. S. *Nano Lett.* **2004**, *4*, 35–39.
- (2) Yao, Z.; Kane, C. L.; Dekker, C. *Phys. Rev. Lett.* **2000**, *84*, 2941–2944.
- (3) Snow, E. S.; Novak, J. P.; Campbell, P. M.; Park, D. *Appl. Phys. Lett.* **2003**, *82*, 2145–2147.
- (4) Xiao, K.; Liu, Y. Q.; Hu, P. A.; Yu, G.; Wang, X. B.; Zhu, D. B. *Appl. Phys. Lett.* **2003**, *83*, 150–152.
- (5) Bradley, K.; Gabriel, J.-C. P.; Grüner, G. *Nano Lett.* **2003**, *3*, 1353–1355.

- (6) Seidel, R.; Graham, A. P.; Unger, E.; Duesberg, G. S.; Liebau, M.; Steinhoegl, W.; Kreupl, F.; Hoenlein, W.; Pompe, W. *Nano Lett.* **2004**, *4*, 831–834.
- (7) Saran, N.; Parikh, K.; Suh, D. S.; Muñoz, E.; Kolla, H.; Manohar, S. K. *J. Am. Chem. Soc.* **2004**, *126*, 4462–4463.
- (8) Guo, Y. Z.; Minami, N.; Kazaoui, S.; Peng, J. B.; Yoshida, M.; Miyashita, T. *Physica B* **2002**, *323*, 235–236.
- (9) Kim, Y.; Minami, N.; Zhu, W. H.; Kazaoui, S.; Azumi, R.; Matsumoto, M. *Jpn. J. Appl. Phys.* **2003**, *42*, 7629–7634.
- (10) Armitage, N. P.; Gabriel, J.-C. P.; Grüner, G. *J. Appl. Phys.* **2004**, *95*, 3228–3230.
- (11) Krstic, V.; Duesberg, G. S.; Muster, J.; Burghard, M.; Roth, S. *Chem. Mater.* **1998**, *10*, 2338–2340.
- (12) Albrecht, P. M.; Lyding, J. W. *Appl. Phys. Lett.* **2003**, *83*, 5029–5031.
- (13) Burghard, M.; Duesberg, G.; Philipp, G.; Muster, J.; Roth, S. *Adv. Mater.* **1998**, *10*, 584–588.
- (14) Choi, K. H.; Bourgoin, J. P.; Auvray, S.; Esteve, D.; Duesberg, G. S.; Roth, S.; Burghard, M. *Surf. Sci.* **2000**, *462*, 195–202.
- (15) Lewenstein, J. C.; Burgin, T. P.; Ribayrol, A.; Nagahara, L. A.; Tsui, R. K. *Nano Lett.* **2002**, *2*, 443–446.
- (16) Liu, J.; Casavant, M. J.; Cox, M.; Walters, D. A.; Boul P.; Lu, W.; Rimberg, A. J.; Smith, K. A.; Colbert, D. T.; Smalley, R. E. *Chem. Phys. Lett.* **1999**, *303*, 125–129.
- (17) Gerdes, S.; Ondarçuhu, T.; Cholet, S.; Joachim, C. *Europhys. Lett.* **1999**, *48*, 292–298.
- (18) Rao, S. G.; Huang, L.; Setyawan, W.; Hong, S. H. *Nature* **2003**, *425*, 36–37.
- (19) Tsukruk, V. V.; Ko, H.; Peleshanko, S. *Phys. Rev. Lett.* **2004**, *92*, 065502-1–065502-4.
- (20) Lay, M. D.; Novak, J. P.; Snow, E. S. *Nano Lett.* **2004**, *4*, 603–606.
- (21) Oh, S. J.; Cheng, Y.; Zhang, J.; Shimoda, H.; Zhou, O. *Appl. Phys. Lett.* **2003**, *82*, 2521–2523.
- (22) Shimoda, H.; Oh, S. J.; Geng, H. Z.; Walker, R. J.; Zhang, X. B.; McNeil, L. E.; Zhou, O. *Adv. Mater.* **2002**, *14*, 899–901.
- (23) Rogers, J. A.; Jackman, R. J.; Whitesides, G. M. *Adv. Mater.* **1997**, *9*, 475.
- (24) Nakao, H.; Gad, M.; Sugiyama, S.; Otobe, K.; Ohtani, T. *J. Am. Chem. Soc.* **2003**, *125*, 7162–7163.
- (25) Gad, M.; Sugiyama, S.; Ohtani, T. *J. Biomol. Struct. Dyn.* **2003**, *21*, 387–393.
- (26) Collins, P. G.; Arnold, M. S.; Avouris, Ph. *Science* **2001**, *292*, 706–709.

NL0491935